Hindawi
Mathematical Problems in Engineering
Volume 2018, Article ID 8239464, 13 pages
https://doi.org/10.1155/2018/8239464

Research Article

The Optimal Design of an Arch Girder of Variable Curvature and Stiffness by Means of Control Theory

Dorota Jasińska and Dorota Kropiowska

Faculty of Civil Engineering, Institute of Structural Mechanics, Cracow University of Technology, Warszawska 24, Cracow 31-155, Poland

Correspondence should be addressed to Dorota Jasińska; djasinska@pk.edu.pl

Received 31 October 2018; Accepted 3 December 2018; Published 24 December 2018

Academic Editor: Mohammad Amin Hariri-Ardebili

The problem of optimal design of the statically indeterminate arch girder which constitutes the primary structural system of the arch bridge is presented. The task is to determine the optimal shape of the axis of the arch girder, as well as the optimal distribution of the cross section height, ensuring the minimum arch volume as well as fulfillment of the standard requirements. This optimisation task, with numerous control functions and constraints, is formulated as a control theory problem with maintaining the formal structure of the minimum principle and then transformed to the multipoint boundary value problem and solved by means of numerical methods. The numerical results are obtained with optimal control methods, using the Dircol software. Since the changes in the shape and cross-section of the arch affect the distribution of the dead and moving loads transferred on the girder from the bridge deck, the optimisation procedure is combined with the finite element method analysis, which together with the complexity of the multidecision arch optimisation problem accounts for the novelty of the proposed approach. The numerical analysis reveals that the optimal girder shape is the frame-arched structure, with considerable lengths of straight sections and only short arch elements, in the areas of the application of concentrated forces and moments. The presented method can be successfully extended to optimisation of structures with different static schemes and load categories taken into account.

1. Introduction

Arches have been widely used as bridge structural elements for centuries. In contemporary engineering, arch girders are highly attractive to designers and architects due to their resistance, safety, and the possibility of shaping their various forms; as a result, they actively influence the landscape. Arch girders are therefore important, expensive, and often unique structural elements of many bridge structures, so the crucial issue is searching for optimal girder shapes and optimal geometry of their cross sections that will reduce construction costs while simultaneously meeting all the constraints arising both from standards and imposed by developers.

The need to take into account all these constraints, as well as many load combinations and control variables significantly increases the dimensions of optimisation problems and complexity of mathematical modelling. This often results in the necessity of task simplification in order to fit into the model.

Some early work on the optimal design of the cross section of the simple arched structures can be found in [1, 2]. Solutions for the optimal shape of the plane-statically determined arches subjected to uniform vertical loads were presented in [3, 4]. Some papers have been published addressing the issue of the shaping of the arch axis and the interesting aesthetic and structural aspects of this matter [5–7]. The buried concrete arch was studied in the paper by Houšt et al. [8], where the optimal shape with regard to the minimisation of the maximal stresses was found. The issue of minimisation of the maximal stress over an arch structure in the context of linear elastic thin shell theory was analysed in [9]. Examples of the determination of the optimum shape of brick masonry arches under dynamic loads by cellular automata were presented by Kumarci et al. [10]. Issues related to the optimal design of a steel arch bridge using a genetic algorithm were presented in [11], where the effectiveness of the optimal design of an arch bridge made of high performance steel was analysed in comparison

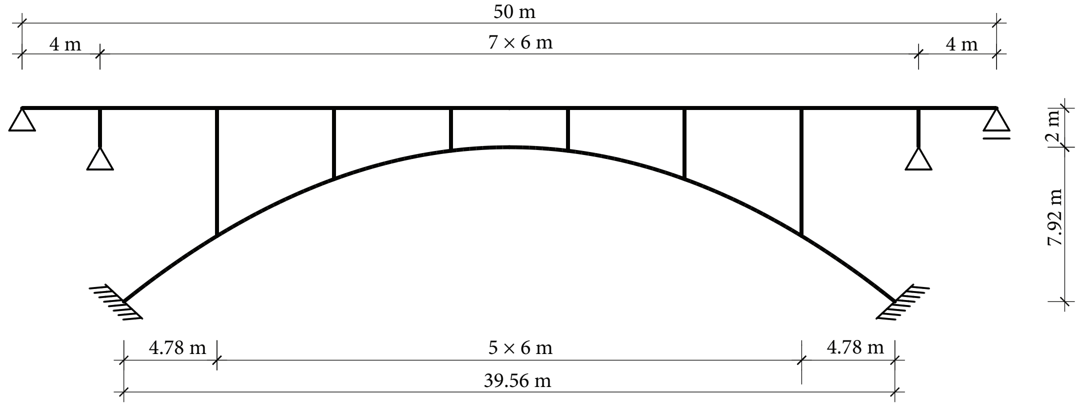

Figure 1: Diagram of the pre-optimisation arch bridge structure.

with a conventional design. The problem concerning the shape optimization of concrete open spandrel arch bridges by the simultaneous perturbation stochastic approximation algorithm was discussed in [12].

However, it can be observed that there are still many unsolved problems related to the discussed topic. A large majority of the research works regarding arch optimisation are only related to the search for an optimal arch axis or only for optimal cross section geometry.

There is a lack of research regarding multidecision optimisation problems that additionally account for many constraints and loads, especially with regards to searching for the optimal curvature of the arch axis. The methods capable of solving such sophisticated structural design optimisation problems are based on the optimal control theory.

Most optimal control problems in engineering are related to time-optimal issues [13]. The use of control theory in the optimal design of structural elements became possible after interesting relationships between shape optimisation and the optimisation of processes were discovered. The defining of optimisation problems of bar elements within the formalism of the Pontryagin minimum principle [14] became particularly possible as a result of adopting an independent variable, namely, the coordinate measured along a bar geometric axis instead of time. Various problems in the optimal design of bar systems have been solved, especially the optimisation of reinforced concrete and steel frames [15], the optimisation of thin-walled beams [16], and multispan girders [16–18].

This paper investigates the more complex optimal design task of a real bridge structure. The application of Pontryagin's minimum principle in combination with FEM computations allow global solutions to design problems to be reached. They provide all the information on shaping a girder of variable curvature and stiffness in a way that guarantees the minimisation of the accepted objective function while simultaneously meeting all the constraints arising from standards and the constraints additionally imposed by developers.

2. Description of the Optimised Structure

The concrete arch under consideration constitutes the primary structural system of the arch bridge. The span length of the arch girder is 39.56 m, its preoptimisation shape is parabolic with a rise of 7.92 m, and the rectangular cross-section dimensions are width $b = 3.5$ m and initial height $h = 0.62$ m. The road has two traffic lanes which are 2.75 m wide, a hard strip and a vehicle parapet (1.2 m wide) on each side. The reinforced concrete deck, 50 m long, with a slab and beam cross section (7.9 × 0.2 m slab, strengthened by three beams 0.6 × 0.4 m), is supported by eight equally spaced columns, six of which are founded in the girder. The column cross sections are 3.5 × 0.55 m. The bridge geometry and dimensions are presented in Figure 1.

For dead load assessment, the following non-structural elements are considered: a safety barrier with a cornice at each side (combined total of 6 kN/m), and the waterproofing and asphalt layers with a combined thickness of 8 cm (2.78 kN/m). The traffic load is represented by a uniform distributed load with a weight density of 60.6 kN/m and the concentrated loads of the tandem (a system of two concentrated axle forces 675 kN each, separated by 1.2 m) according to EN 1991-2 [19]. Wind and thermal actions on the bridge are not taken into account.

In order to identify the least favourable load combinations, the whole bridge structure is initially analysed in the Abaqus FEM code. The FEM model of the bridge is constructed from linear Euler-Bernoulli beam elements (to adjust the beam model to the conditions decided for the optimisation problem). The number of beam elements is around 1300. All discussed loads are considered with arbitrary positions of tandem forces.

The ten tandem positions giving the most extreme stresses in the arch girder are identified out of a possible eighty-two, and the appropriate loads from the column footings are transferred to the arch in the form of normal and tangential forces and bending moments (Figure 2). The girder is also subjected to self-weight. The global system (x, y, z) consists of the principal central axes of inertia.

The geometry of the arch cross section as well as the shape of the arch axis is subjected to optimisation. The curvature of the arch axis is controlled, thus allowing any shape for the optimal arch girder, assuming a fixed position for the end supports (characteristic points P_0 and P_7) and fixed

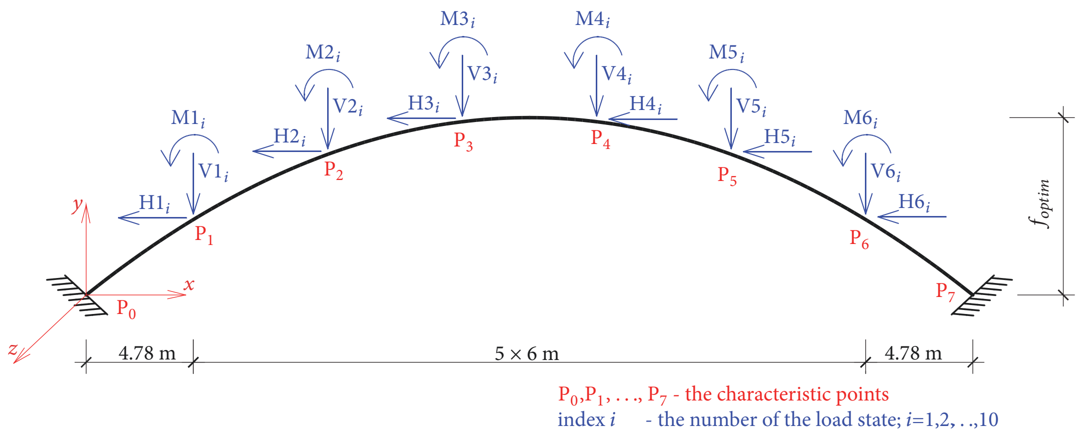

Figure 2: Diagram of the arch girder with loads.

spans between the columns. The eight characteristic points determine seven characteristic intervals.

In comparison to the initial girder, the rise of the optimal arch axis and its cross-sectional characteristics are altered. This automatically leads to changes in the length of the six columns and in the structure's stiffness. Thus, the whole bridge structure model with the optimal arch shape is analysed once more by FEM, and verified for both ultimate and serviceability limit states.

In the mathematical model developed for the optimisation problem under discussion, the use of linear elastic material and slightly curved bars is assumed and Bernoulli's principle (plane cross section assumption) is applied. The considerations are limited to the arch axis, assuming that both it and the load lie in the same plane overlaying the main bending plane and that the system is protected against stability loss. The girder is assumed to be homogenous and made of reinforced concrete, with elastic modulus $E = 30$ GPa and specific weight $\gamma = 25\,\text{kN/m}^3$.

3. Formulation of the Optimal Control Problem

The optimisation problem is defined as the search for the optimal shape of the girder axis and the optimal distribution of the height of the cross section that minimises the assumed objective function, while meeting all the constraint conditions.

Elements of the formal structure of the optimal control problem in question are state equations, boundary conditions and internal point conditions, constraint conditions, and the objective function.

3.1. State Equations. State equations are defined by means of a system of first order ordinary differential equations and provide relationships between state variables, control variables, and structural parameters. Control and state variables are functions of the independent variable x and can be discontinuous in a finite number of points. The state variables may be adopted as components of an internal force vector, components of a displacement vector, components of a strain state, and components of a stress state. The structural parameters depend on geometric and physical properties of a structure.

The mathematical model of the analysed arch girder with a variable axis curvature is developed and arranged as a set of nine first-order differential equations (1) [16, 20, 21]:

$$\begin{aligned}
\frac{\mathrm{d}N}{\mathrm{d}x} &= -Q \cdot \frac{\kappa}{\cos\theta} - \frac{q_s}{\cos\theta} \\
\frac{\mathrm{d}Q}{\mathrm{d}x} &= N \cdot \frac{\kappa}{\cos\theta} - \frac{q_n}{\cos\theta} \\
\frac{\mathrm{d}M}{\mathrm{d}x} &= \frac{Q}{\cos\theta} \\
\frac{\mathrm{d}u}{\mathrm{d}x} &= \frac{N}{E \cdot A \cdot \cos\theta} + w \cdot \frac{\kappa}{\cos\theta} \\
\frac{\mathrm{d}w}{\mathrm{d}x} &= -u \cdot \frac{\kappa}{\cos\theta} + \frac{\varphi}{\cos\theta} \\
\frac{\mathrm{d}\varphi}{\mathrm{d}x} &= \frac{M}{E \cdot I_z \cdot \cos\theta} \\
\frac{\mathrm{d}y}{\mathrm{d}x} &= tg\theta \\
\frac{\mathrm{d}\theta}{\mathrm{d}x} &= \frac{\kappa}{\cos\theta} \\
\frac{\mathrm{d}V}{\mathrm{d}x} &= \frac{A}{\cos\theta}
\end{aligned} \tag{1}$$

where N is axial force; Q is transverse force; M is bending moment; u is displacement tangent to the girder axis; w is displacement perpendicular to the girder axis; φ is angular displacement; y is girder axis coordinate; θ is the inclination angle of the girder axis towards axis x; V is total volume of material of the girder; q_s and q_n are continuous loads in directions tangent and normal to the axis, respectively.

Two control variables are implemented: the first is assumed as the girder axis curvature $U_1 = \kappa$, the second, as the girder cross-section height $U_2 = h$.

Constraints for the trajectories of control variables are also imposed:

$$U_{1\ \mathrm{min}} \leq U_1 \leq U_{1\ \mathrm{max}} \tag{2}$$

$$U_{2\ \mathrm{min}} \leq U_2 \leq U_{2\ \mathrm{max}} \tag{3}$$

The girder's cross section area and its moment of inertia may be defined from the relations:

$$\begin{aligned} A &= b \cdot U_2, \\ I_z &= \frac{b \cdot U_2{}^3}{12} \end{aligned} \tag{4}$$

Given that all ten load states have to be considered, sixty-three state variables are defined, six state variables (N, Q, M, u, w, φ) for each load state $i = 1, 2, \ldots 10$, respectively, and three state variables that define the shape of the girder axis and its total volume (y, θ, V).

Eventually, a set of sixty-three state equations is defined separately for each characteristic intervals in the form of (5).

$$\begin{aligned} \frac{\mathrm{d}N_i}{\mathrm{d}x} &= -Q_i \cdot \frac{U_1}{\cos\theta} + \gamma \cdot b \cdot U_2 \cdot \tan\theta \\ \frac{\mathrm{d}Q_i}{\mathrm{d}x} &= N_i \cdot \frac{U_1}{\cos\theta} - \gamma \cdot b \cdot U_2 \\ \frac{\mathrm{d}M_i}{\mathrm{d}x} &= \frac{Q_i}{\cos\theta} \\ \frac{\mathrm{d}u_i}{\mathrm{d}x} &= \frac{N_i}{E \cdot b \cdot U_2 \cdot \cos\theta} + w_i \cdot \frac{U_1}{\cos\theta} \\ \frac{\mathrm{d}w_i}{\mathrm{d}x} &= -u_i \cdot \frac{U_1}{\cos\theta} + \frac{\varphi_i}{\cos\theta} \\ \frac{\mathrm{d}\varphi_i}{\mathrm{d}x} &= \frac{12 M_i}{E \cdot b \cdot U_2{}^3 \cdot \cos\theta} \\ \frac{\mathrm{d}y}{\mathrm{d}x} &= tg\theta \\ \frac{\mathrm{d}\theta}{\mathrm{d}x} &= \frac{U_1}{\cos\theta} \\ \frac{\mathrm{d}V}{\mathrm{d}x} &= \frac{b \cdot U_2}{\cos\theta} \\ & \text{for } i = 1, 2, \ldots, 10 \end{aligned} \tag{5}$$

3.2. Boundary Conditions and Interior Point Conditions. Boundary conditions and interior point conditions result from the manner in which the arch girder is supported and loaded by concentrated forces and moments. In general, for the task under discussion, 441 (63×7) conditions are defined. They comprise the 321 explicit conditions listed in Table 1 and 120 implicit conditions.

Implicit conditions are defined for state variables N_i and Q_i for each load state $i = 1, 2, \ldots 10$, and result from the need to take into account all concentrated forces applied to the characteristic points P_1 to P_6. The 120 implicit conditions are defined in accordance with (6).

$$\begin{aligned} & N_i^+ - N_i^- - \mathrm{V1}_i \cdot \sin(\theta) - \mathrm{H1}_i \cdot \cos(\theta) = 0 \\ & Q_i^+ - Q_i^- + \mathrm{V1}_i \cdot \cos(\theta) - \mathrm{H1}_i \cdot \sin(\theta) = 0 \\ & N_i^+ - N_i^- - \mathrm{V2}_i \cdot \sin(\theta) - \mathrm{H2}_i \cdot \cos(\theta) = 0 \\ & Q_i^+ - Q_i^- + \mathrm{V2}_i \cdot \cos(\theta) - \mathrm{H2}_i \cdot \sin(\theta) = 0 \\ & N_i^+ - N_i^- - \mathrm{V3}_i \cdot \sin(\theta) - \mathrm{H3}_i \cdot \cos(\theta) = 0 \\ & Q_i^+ - Q_i^- + \mathrm{V3}_i \cdot \cos(\theta) - \mathrm{H3}_i \cdot \sin(\theta) = 0 \\ & \qquad \text{for each: } i = 1, 2, \ldots, 10 \\ & N_i^+ - N_i^- - \mathrm{V4}_i \cdot \sin(\theta) - \mathrm{H4}_i \cdot \cos(\theta) = 0 \\ & Q_i^+ - Q_i^- + \mathrm{V4}_i \cdot \cos(\theta) - \mathrm{H4}_i \cdot \sin(\theta) = 0 \\ & N_i^+ - N_i^- - \mathrm{V5}_i \cdot \sin(\theta) - \mathrm{H5}_i \cdot \cos(\theta) = 0 \\ & Q_i^+ - Q_i^- + \mathrm{V5}_i \cdot \cos(\theta) - \mathrm{H5}_i \cdot \sin(\theta) = 0 \\ & N_i^+ - N_i^- - \mathrm{V6}_i \cdot \sin(\theta) - \mathrm{H6}_i \cdot \cos(\theta) = 0 \\ & Q_i^+ - Q_i^- + \mathrm{V6}_i \cdot \cos(\theta) - \mathrm{H6}_i \cdot \sin(\theta) = 0 \end{aligned} \tag{6}$$

In addition, it is necessary to define explicit interior point conditions for control variables (Table 2).

3.3. Objective Function. In the case of structural optimal design, different optimisation criteria may be adopted. The strength criterion is adopted in problems concerning minimization of maximum deflections, maximum bending moments or maximum normal stress. Other criteria concern the cost of constructing the engineering structure. The material costs can be included by assuming the volume of the structure as an objective function. However, the costs of construction processes for optimally shaped elements are difficult to define clearly. Thus, they are mostly not considered in an objective function. Therefore, when assuming structure volume as a function which will be minimised in the optimisation task, efforts should be made to find an optimal solution which will not generate significant costs in construction.

For the problem under discussion, volume minimisation is assumed as an optimisation criterion. The optimal control problem of the Lagrange functional in the form (7)

$$J(\mathbf{X}(x), \mathbf{U}(x)) = \int_0^{x_{P7}} \frac{A}{\cos\theta} \mathrm{d}x \tag{7}$$

is transformed, thanks to the introduction of the state equation $\mathrm{d}V/\mathrm{d}x = A/\cos\theta$, into a Mayer problem with functional (8) and initial condition (9):

$$J(\mathbf{X}(x), \mathbf{U}(x)) = V(\mathbf{X}(x_{P7}), \mathbf{U}(x_{P7})) \tag{8}$$

$$V(\mathbf{X}(0), \mathbf{U}(0)) = 0 \tag{9}$$

where $\mathbf{X}(x), \mathbf{U}(x)$ are vectors of state variables and control variables, respectively.

TABLE 1: Boundary conditions and explicit interior point conditions for state variables.

State variable for each $i = 1, 2 \ldots, 10$	**Characteristic point**													
	$\mathbf{P_0}$	$\mathbf{P_1}$		$\mathbf{P_2}$		$\mathbf{P_3}$		$\mathbf{P_4}$		$\mathbf{P_5}$		$\mathbf{P_6}$		$\mathbf{P_7}$
		Left (-)	Right (+)	Left (-)	Right (+)	Left (-)	Right (+)	Left (-)	Right (+)	Left (-)	Right (+)	Left (-)	Right (+)	
$\boldsymbol{N_i}$	-	-	-	-	-	-	-	-	-	-	-	-	-	-
$\boldsymbol{Q_i}$	-	-	-	-	-	-	-	-	-	-	-	-	-	-
$\boldsymbol{M_i}$	-	$M_i^- = M_i^+ + \mathrm{M1}_i$		$M_i^- = M_i^+ + \mathrm{M2}_i$		$M_i^- = M_i^+ + \mathrm{M3}_i$		$M_i^- = M_i^+ + \mathrm{M4}_i$		$M_i^- = M_i^+ + \mathrm{M5}_i$		$M_i^- = M_i^+ + \mathrm{M6}_i$		-
$\boldsymbol{u_i}$	0	$u_i^- = u_i^+$		$u_i^- = u_i^+$		$u_i^- = u_i^+$		$u_i^- = u_i^+$		$u_i^- = u_i^+$		$u_i^- = u_i^+$		0
$\boldsymbol{w_i}$	0	$w_i^- = w_i^+$		$w_i^- = w_i^+$		$w_i^- = w_i^+$		$w_i^- = w_i^+$		$w_i^- = w_i^+$		$w_i^- = w_i^+$		0
$\boldsymbol{\varphi_i}$	0	$\varphi_i^- = \varphi_i^+$		$\varphi_i^- = \varphi_i^+$		$\varphi_i^- = \varphi_i^+$		$\varphi_i^- = \varphi_i^+$		$\varphi_i^- = \varphi_i^+$		$\varphi_i^- = \varphi_i^+$		0
$\boldsymbol{y}$	0	$y^- = y^+$		$y^- = y^+$		$y^- = y^+$		$y^- = y^+$		$y^- = y^+$		$y^- = y^+$		0
$\boldsymbol{\theta}$	-	$\theta^- = \theta^+$		$\theta^- = \theta^+$		$\theta^- = \theta^+$		$\theta^- = \theta^+$		$\theta^- = \theta^+$		$\theta^- = \theta^+$		-
$\boldsymbol{V}$	0	$V^- = V^+$		$V^- = V^+$		$V^- = V^+$		$V^- = V^+$		$V^- = V^+$		$V^- = V^+$		-

TABLE 2: Explicit interior point conditions for control variables.

Control variable	Characteristic point													
	P_0	P_1		P_2		P_3		P_4		P_5		P_6		P_7
		Left (-)	Right (+)	Left (-)	Right (+)	Left (-)	Right (+)	Left (-)	Right (+)	Left (-)	Right (+)	Left (-)	Right (+)	
$\boldsymbol{U_1 = \kappa}$	-	$\kappa^- = \kappa^+$		$\kappa^- = \kappa^+$		$\kappa^- = \kappa^+$		$\kappa^- = \kappa^+$		$\kappa^- = \kappa^+$		$\kappa^- = \kappa^+$		-
$\boldsymbol{U_2 = h}$	-	$h^- = h^+$		$h^- = h^+$		$h^- = h^+$		$h^- = h^+$		$h^- = h^+$		$h^- = h^+$		-

3.4. Constraint Conditions. The inequality constraint conditions result from the need to meet the ultimate and serviceability limit states.

For the optimisation task under discussion, two inequality constraint conditions resulting from the limits of maximum normal stresses and displacements are implemented in the numerical calculation by the Dircol software, which takes into account the ten least favourable load states. Additionally, verification calculations for the whole bridge structure with the optimal arch girder are performed in the Abaqus FEM code each time after receiving the optimal solution. The purpose of these calculations is to verify the limit states for the optimal structure with regard to all eighty-two possible load states. The limit value of normal compressive stresses is assumed to be 13.3 MPa, and the value of allowable vertical displacement is set as 0.132 m.

The first constraint condition in the optimisation task refers to the limit of maximum normal compressive stresses:

$$g_1 = \sigma_0 - \max|\sigma_{xc}| \geq 0 \tag{10}$$

where σ_0 is allowable normal compressive stress, which will not cause the ultimate limit state to be exceeded.

Normal stresses are defined in lower fibres σ_l, in accordance with (11) and upper fibres σ_u (12) for each load state:

$$\sigma_{li} = \frac{N_i}{A} + \frac{M_i}{I_z} \cdot \frac{U_2}{2} \quad \text{for each: } i = 1, 2, \ldots, 10 \tag{11}$$

$$\sigma_{ui} = \frac{N_i}{A} - \frac{M_i}{I_z} \cdot \frac{U_2}{2} \quad \text{for each: } i = 1, 2, \ldots, 10 \tag{12}$$

The envelopes of maximum and minimum normal stresses in lower and upper fibres out of all load states are calculated:

$$\begin{aligned} \max\sigma_l &= \max(\sigma_{li}) \quad \text{for } i = 1, 2, \ldots, 10 \\ \max\sigma_u &= \max(\sigma_{ui}) \end{aligned} \tag{13}$$

$$\begin{aligned} \min\sigma_l &= \min(\sigma_{li}) \quad \text{for } i = 1, 2, \ldots, 10 \\ \min\sigma_u &= \min(\sigma_{ui}) \end{aligned} \tag{14}$$

The envelope of maximum normal compressive stresses is determined from relation (15):

$$\max|\sigma_{xc}| = \max(|\min\sigma_l|, |\min\sigma_u|) \tag{15}$$

The envelope of maximum normal tensile stresses may also be calculated, to help design an appropriate reinforcement for the reinforced concrete element.

The second inequality type constraint condition is related to the maximum vertical displacement limit:

$$g_2 = W_0 - \max W \geq 0 \tag{16}$$

where W_0 is allowable vertical displacement.

Vertical displacement W is defined for each load state in relation (17).

$$W_i = |u_i \cdot \sin\theta + w_i \cdot \cos\theta| \quad \text{for } i = 1, 2, \ldots, 10 \tag{17}$$

An envelope of maximum vertical displacement of all load states is calculated:

$$\max W = \max(W_i) \quad \text{for } i = 1, 2, \ldots, 10 \tag{18}$$

The search for the arch girder with an optimally shaped axis and an optimal cross-section geometry is carried out for various initial assumptions regarding permissible limit values of the control variables $U_{1\,\min}, U_{1\,\max}, U_{2\,\min}, U_{2\,\max}$ in order to find an optimal solution with the smallest value of the objective function.

In view of the assumption that slightly curved bars are being considered restrictions must be placed on the proportion of the lateral cross-section dimension h to the radius of curvature R. The influence of a strong axis curvature may be ignored below the limit value of $h / R = 0.2$ [20, 21]. Based on this condition, for an arch axis with a negative curvature, we impose the limit values of the control variables $U_{1\,\min}$ as: $U_{1\,\min} = -0.3\,\mathrm{m}^{-1}$. Other permissible limit values of the control variables are provided in the next section.

The strong axis curvature effect can also be incorporated in the optimization task; this issue was analysed in our earlier work on different theoretical examples [16].

4. Optimal Solution and Numerical Results

Optimal controls are determined in accordance with the Pontryagin minimum principle. For the objective function and provided constraints, the Hamilton function and the adjoint equations are defined for each characteristic interval. The boundary conditions for the adjoint variables result from the transversality conditions.

The Hamilton function for the problem under discussion is linearly dependent on the control variable U_1 and, for this reason, it is necessary to produce constraints on the control U_1 in the form of (2). In a case of the irregular Hamilton function, singular control or bang-bang control may be obtained for the control variable U_1. At the same

TABLE 3: Comparison of the most important results for the initial task and optimisation tasks 1-4.

Task no.	Arch axis curvature κ [m^{-1}]	Cross-section height h [m]	Rise of an arch f [m]	Volume of concrete V [m^3]	Percentage of material savings [%]
0. (initial task)	parabolic arch, not optimal $-0.0404860 \le \kappa \le -0.0192541$	$h = const$ $h = 0.62$	7.92	94.294	-
1.	$\kappa = U_1$ $-0.04 \le U_1 \le -0.02$	$h = U_2$ $0.5 \le U_2 \le 0.7$	5.56	75.684	19.74
2.	$\kappa = U_1$ $-0.04 \le U_1 \le -0.02$	$h = U_2$ $0.45 \le U_2 \le 0.7$	5.97	69.812	25.96
3.	$\kappa = U_1$ $-0.3 \le U_1 \le -0.02$	$h = U_2$ $0.5 \le U_2 \le 0.7$	5.74	75.596	19.83
4.	$\kappa = U_1$ $-0.3 \le U_1 \le -0.02$	$h = U_2$ $0.45 \le U_2 \le 0.7$	6.36	69.361	26.44

time, there is no linear dependency of the Hamiltonian on the control variable U_2.

The optimal control task is transformed into a multipoint boundary value problem. In order to find the solution to a multipoint boundary value problem for the arch optimisation task, the numerical methods are applied. Among the numerical calculation methods, a direct method is chosen, since it allows for the solution of complex multi-interval tasks. The software based on direct methods, used in discussed problems, is the Dircol 2.1 program: "A Direct Collocation Method for the Numerical Solution of Optimal Control Problems" [22, 23]. Dircol is based on the direct collocation method; the infinite dimensional optimal control problem is transcribed into a sequence of nonlinearly constrained optimization problems (NLPs) by a discretization of state and control variables. The NLPs are solved by means of the sequential quadratic programming (SQP).

The optimal solutions meeting all necessary optimality conditions are found for a number of optimisation tasks with various assumptions regarding permissible limit values of the control variables.

The selection of appropriate limits for control variables starts with the analysis of the initial girder with parabolic arch axis with the rise of $f = 7.92$ m and a constant initial height of $h = 0.62$ m (the minimal value for which the ultimate limit state is fulfilled).

From among the numerous carried out calculations, solutions of the eight most interesting examples are presented in this article. The first two optimisation tasks deal with the search for optimal solutions within the range of permissible values of the curvature which are close to the range of the curvature of the initial parabolic arch, i.e. $-0.04\,m^{-1} \le \kappa \le -0.02\,m^{-1}$. The possible courses for the optimal girder height are adopted as: $0.5\,m \le h \le 0.7\,m$ for task no. 1, and $0.45\,m \le h \le 0.7\,m$ for task no. 2. As expected, a slight extension of the range of permissible values of the girder height for task no. 2 enabled obtaining a solution characterised by a smaller value of the objective function (Table 3). A further reduction of the permissible minimum height h_{min} is not possible due to the need to fulfil technological and design requirements.

For the remaining tasks the allowable values of curvature are not so strictly limited. For tasks 3 and 4, the lower curvature limit is reduced to the minimal value satisfying the condition for slightly curved bars. From cases 1 to 4 the one with the smallest value of the objective function is further expanded upon in tasks 5-8, where the impact of the upper curvature limit is analysed.

The calculation results are obtained for each optimisation task as a set of numerical data and in graphic form as diagrams of sixty-three state variables, sixty-three adjoint variables, two control variables, the Hamilton function, and two constraint conditions, inter alia. All conditions for the adjoint variables resulting from the transversality conditions are met. The optimal distributions of the control variables providing the minimisation of the material volume are obtained for each optimisation task. Because of the Hamilton function's linear dependency on control U_1, singular solutions are found, and also the control variable U_1 takes values from the boundary of the allowable area. The most important results obtained for the first four optimisation tasks are listed in Table 3.

The implementation of two control variables, these being the arch axis curvature and cross-section height, makes it possible to obtain a significant minimisation of the objective function while simultaneously meeting the ultimate and serviceability limit states for the whole bridge structure. The volume of material for the arch girder is reduced from approximately 94 m^3 for the initial task, to 69 m^3 for task no. 4. The optimal arches are also less elevated than the original one. The diagrams of the optimal distribution of the girder height, the optimal curvature, and the corresponding shape of an arch girder axis and the course of inclination angle for tasks 3 and 4 are set out in Figures 3–6.

Optimal height distributions for each of the four obtained solutions show a significant increase of height in the area of the application of concentrated forces and moments. For each task, this height is shaped differently depending, inter alia, on the optimal distribution of curvature.

The whole bridge structure model with each of the four optimal girders is analysed once more by FEM and checked

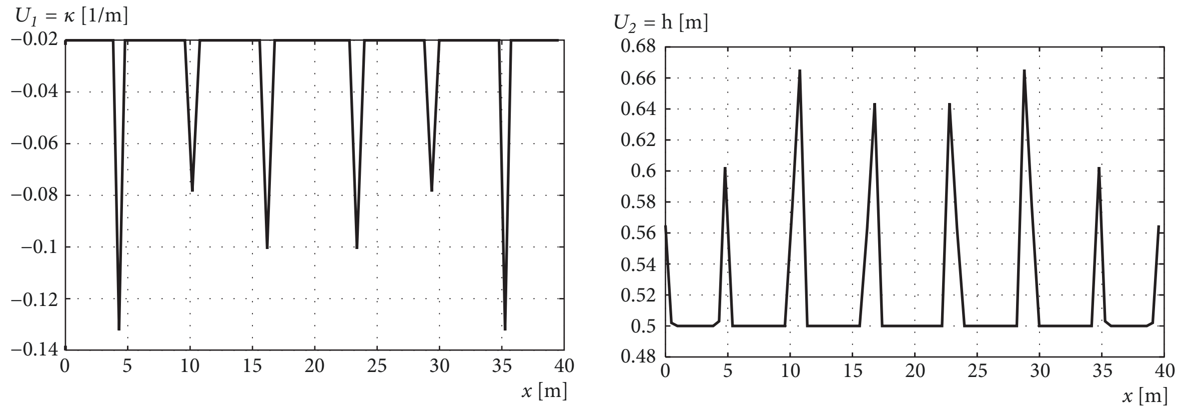

Figure 3: Control variables for task no. 3.

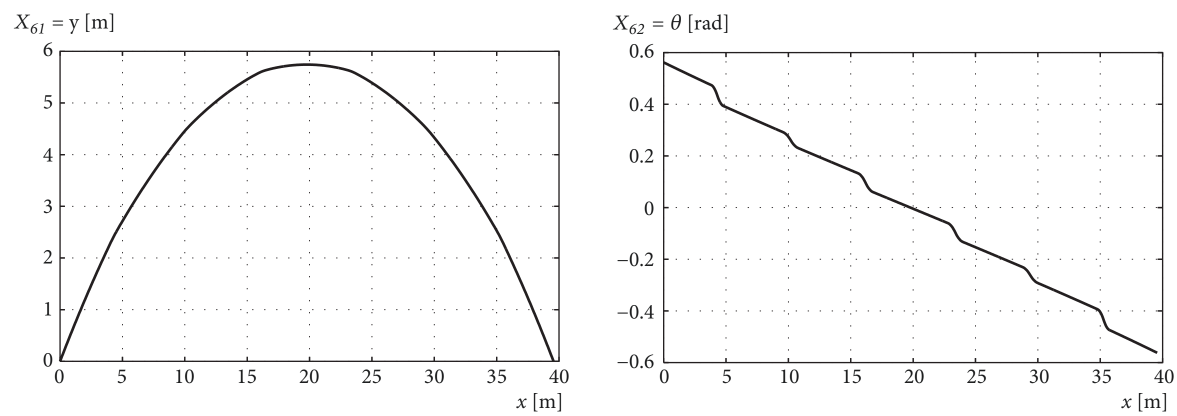

Figure 4: Optimal arch axis shape and corresponding optimal inclination angle for task no. 3.

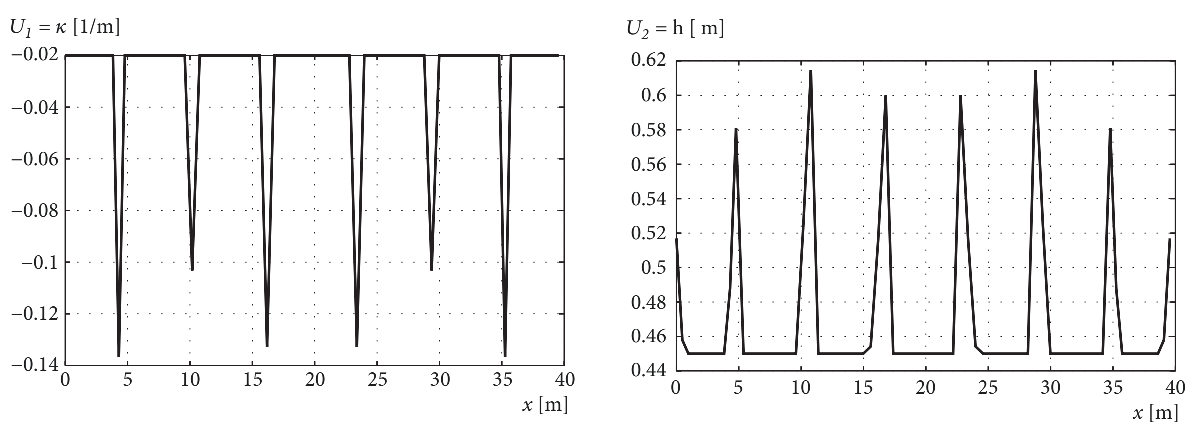

Figure 5: Control variables for task no. 4.

for both ultimate and serviceability limit states. The stress and deflection envelopes for the initial and optimal arches are presented in Figures 7–11.

A considerable change in the distribution of the compressive stress envelopes can be observed. The stresses values are significantly closer to the allowable stress for the optimally shaped girder than for the initial task. Due to the necessity of taking into account all eighty-two load states and the fulfillment of ultimate and serviceability limit states for each of these load states, it is not possible to obtain a distribution of normal stresses along the entire length of the arch close to the allowable value. Deflections for the optimal and therefore lighter arch increase but do not exceed the limit value.

In order to find the optimal solution with the smallest value of the objective function, the calculations of four additional tasks are carried out, with expanded upper curvature limits, as shown in Table 4.

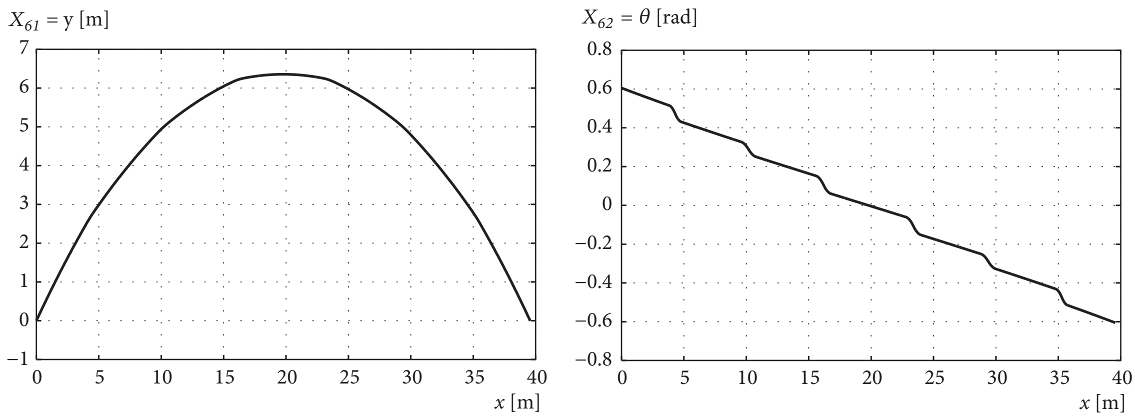

Figure 6: Optimal arch axis shape and corresponding optimal inclination angle for task no. 4.

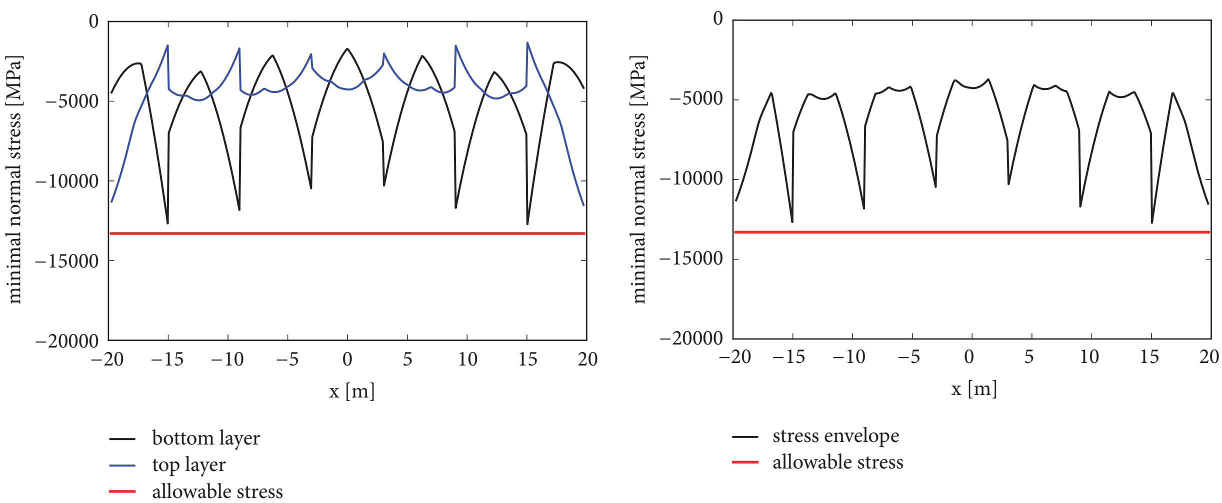

Figure 7: The stress envelopes by Abaqus FEM code for the initial task.

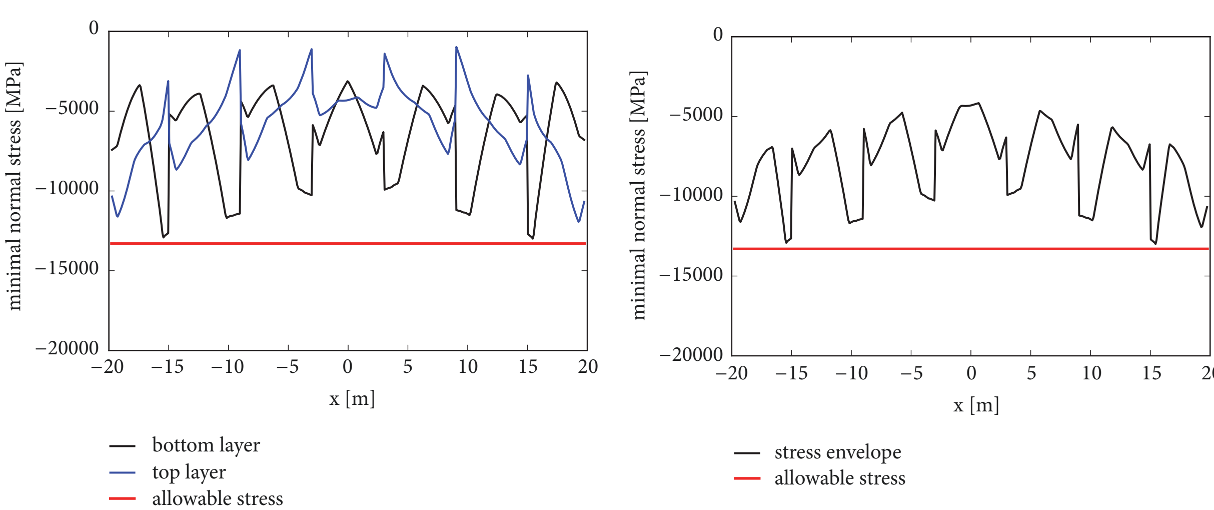

Figure 8: The stress envelopes by Abaqus FEM code for task no. 3.

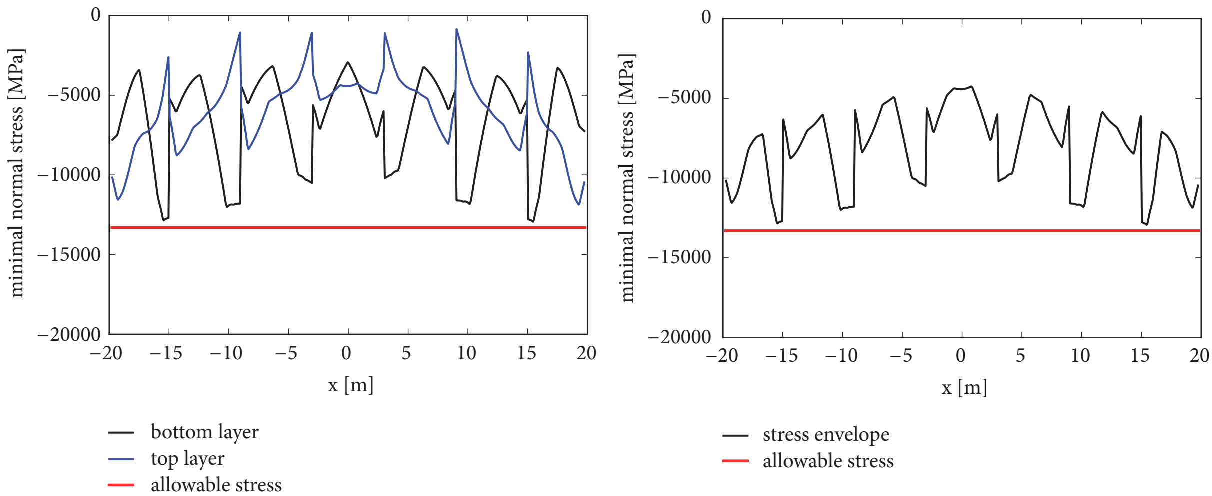

Figure 9: The stress envelopes by Abaqus FEM code for task no. 4.

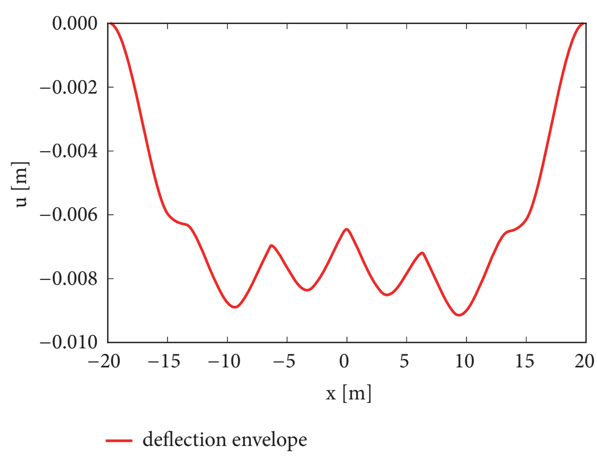

Figure 10: The deflection envelope by Abaqus FEM code for the initial task.

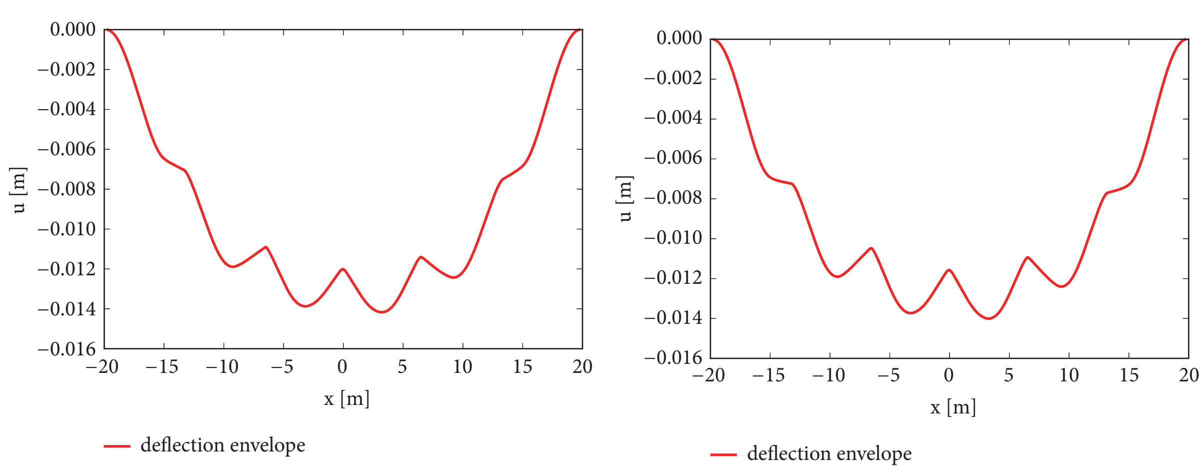

Figure 11: The deflection envelopes by Abaqus FEM code for task no. 3 (left) and no. 4 (right).

Table 4: Comparison of the most important results for the next optimisation tasks.

Task no.	Arch axis curvature κ $[\mathrm{m}^{-1}]$	Cross-section height h [m]	Rise of an arch f [m]	Volume of concrete V $[\mathrm{m}^3]$	Percentage of material savings [%]
5.	$\kappa = U_1$ $-0.3 \le U_1 \le -0.015$	$h = U_2$ $0.45 \le U_2 \le 0.7$	6.17	69.035	26.79
6.	$\kappa = U_1$ $-0.3 \le U_1 \le -0.01$	$h = U_2$ $0.45 \le U_2 \le 0.7$	6.06	68.873	26.96
7.	$\kappa = U_1$ $-0.3 \le U_1 \le -0.005$	$h = U_2$ $0.45 \le U_2 \le 0.7$	5.68	68.664	27.18
8.	$\kappa = U_1$ $-0.3 \le U_1 \le 0$	$h = U_2$ $0.45 \le U_2 \le 0.7$	5.54	68.369	27.49

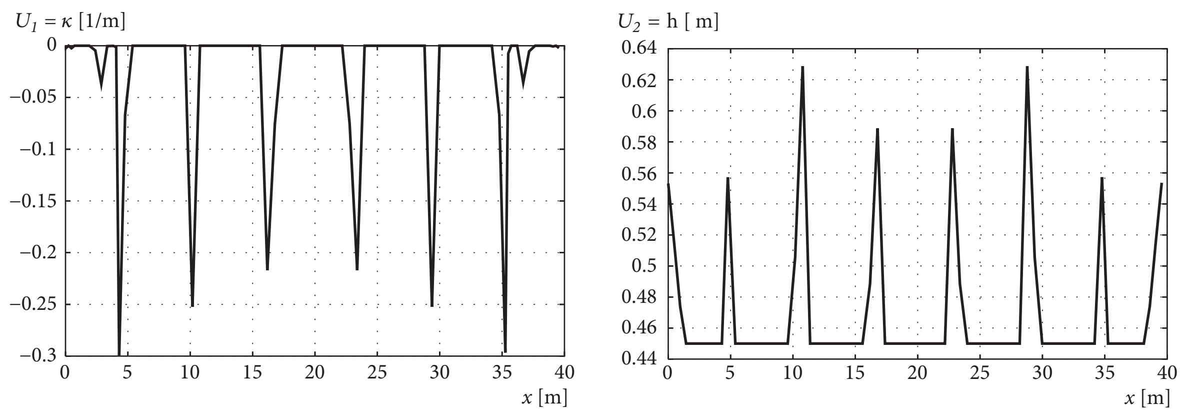

Figure 12: Control variables for task no. 8.

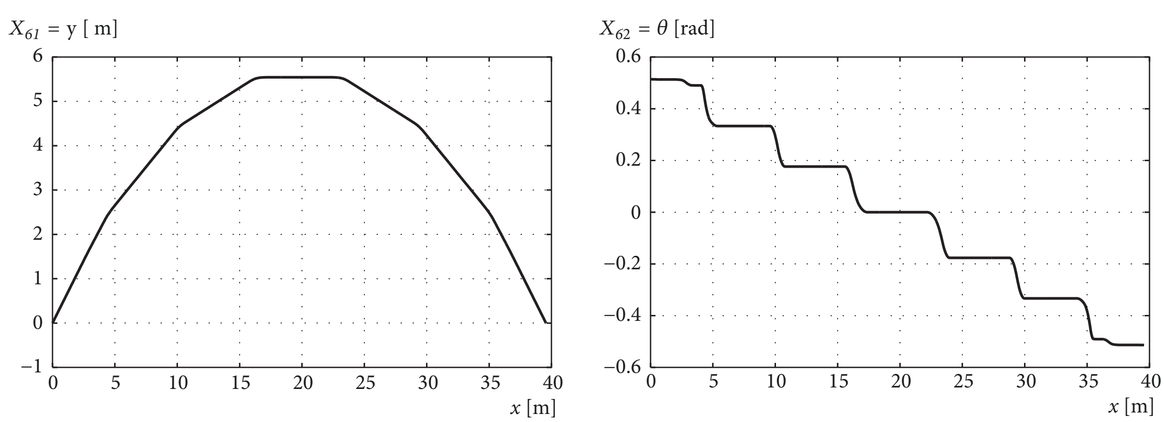

Figure 13: Optimal girder axis shape and corresponding optimal inclination angle for task no. 8.

Comparing the volume obtained for the optimally shaped girder for the best task, no. 8 ($V = 68.369\,\mathrm{m}^3$), with the value obtained for the initial arch ($V = 94.294\,\mathrm{m}^3$), it can be seen that the objective function has been reduced by over 27%.

The set of the most important diagrams for task number 8 with the smallest value of objective function is shown in Figures 12–14.

As mentioned in the previous section, efforts should be made to find an optimal solution which will not generate significant costs in construction. For the optimisation problem under discussion, the optimal solution of task no. 8 with the minimum volume of material is also the solution that is the simplest in its construction. The optimally shaped girder for that task is a frame-arched girder which has a considerable length of straight sections with short arch elements in the areas of the application of concentrated forces and moments.

As in previous tasks, the whole bridge structure with each of the optimal girders is verified for ultimate and serviceability limit states by Abaqus FEM code. The stress and deflection envelopes for the optimal arch with the smallest value of the objective function are presented in Figures 15 and 16.

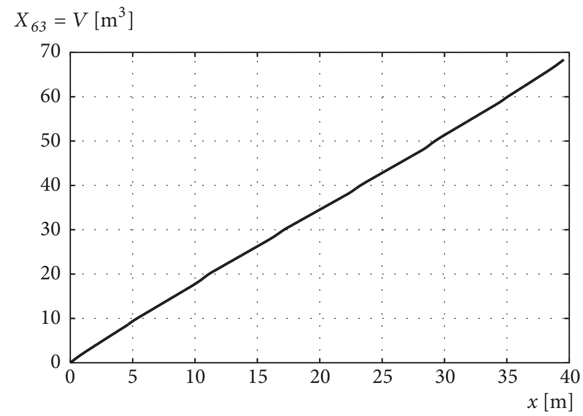

FIGURE 14: Volume of material for task no. 8.

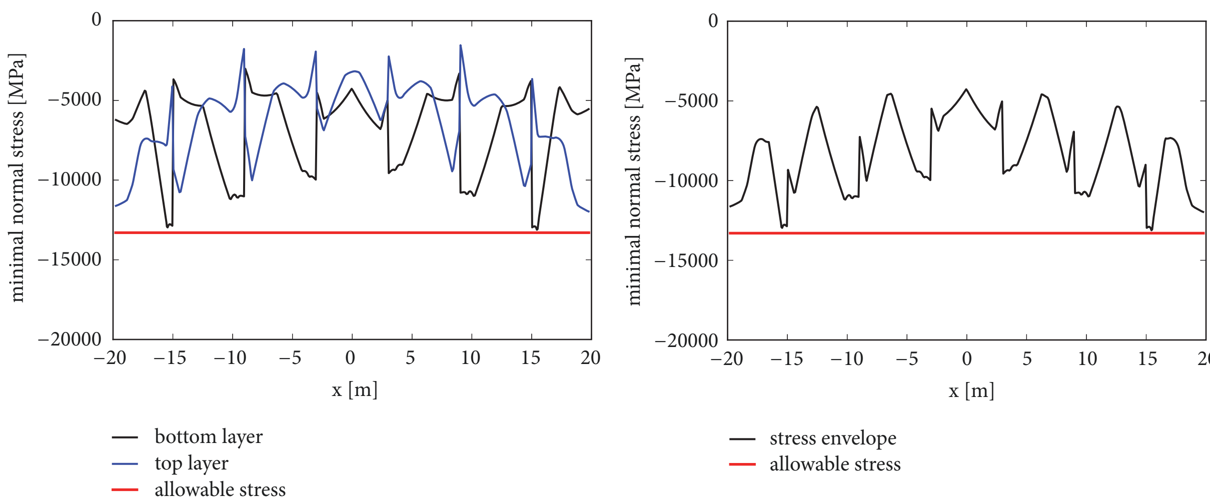

FIGURE 15: The stress envelopes by Abaqus FEM code for task no. 8.

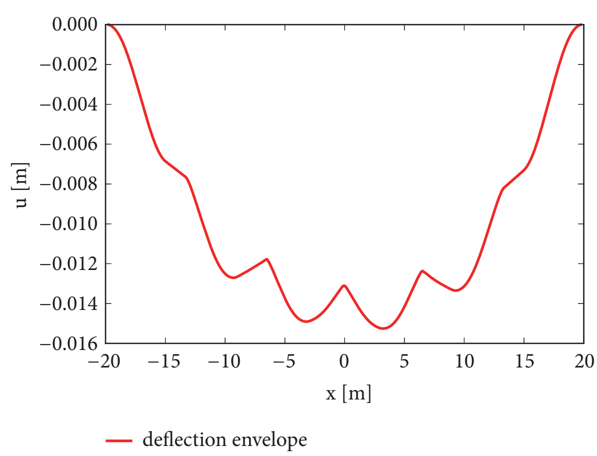

FIGURE 16: The deflection envelopes by Abaqus FEM code for task no. 8.

5. Conclusions

In this paper, a method of optimal design of an arch girder of variable curvature and stiffness by means of control theory is presented. The methodology is based on the application of Pontryagin's minimum principle in combination with FEM computations. The objective is to minimise the total volume of girder's material while simultaneously meeting all constraint conditions. The solutions meeting all necessary optimality conditions are found for numerous tasks.

The trajectories of all state variables, adjoint variables, the Hamilton function, and symmetrical optimal solutions prove the correctness of the obtained results. It should also be emphasised that singular control of the optimal design task is obtained, which is particularly interesting for a problem of such complexity in the context of control theory.

Based on the formulations presented in this article, calculations for various real structures can be performed. The method of the optimal design of the girder with minimal volume can be successfully extended to the optimisation tasks of structures with various static schemes, load states, and other objective functions or boundary conditions. The obtained results confirm that the optimisation method, based on the optimal control theory in combination with FEM computations, can be used successfully in calculations for complex structural systems.

Data Availability

The data used to support the findings of this study are included within the article.

Conflicts of Interest

The authors declare that there are no conflicts of interest regarding the publication of this paper.

Acknowledgments

This work was funded by the Cracow University of Technology, Poland.

References

[1] G. Szefer and L. Mikulski, "Optimal design of elastic arches with I cross-section," *Engineering Transactions*, vol. 32, no. 4, pp. 467–480, 1984.

[2] G. Szefer and L. Mikulski, "Optimal design of elastic arches with rectangular cross section," *SM archives*, vol. 10, no. 2, pp. 171–185, 1985.

[3] G. C. Marano, F. Trentadue, and F. Petrone, "Optimal arch shape solution under static vertical loads," *Acta Mechanica*, vol. 225, no. 3, pp. 679–686, 2014.

[4] F. Trentadue, G. C. Marano, I. Vanzi, and B. Briseghella, "Optimal arches shape for single-point-supported deck bridges," *Acta Mechanica*, vol. 229, no. 5, pp. 2291–2297, 2018.

[5] M. Farshad, "On optimal form of arches," *Journal of The Franklin Institute*, vol. 302, no. 2, pp. 187–194, 1976.

[6] C. Hu, Y. Wan, and X. ShangGuan, "A new practice in the design of arch axis," in *Proceedings of the 6th International Conference on Arch Bridges*, pp. 709–715, Fuzhou University, China, 2010.

[7] R. Osserman, "How the Gateway Arch got its shape," *Nexus Network Journal*, vol. 12, no. 2, pp. 167–189, 2010.

[8] V. Houšt, J. Eliáš, and L. Miča, "Shape optimization of concrete buried arches," *Engineering Structures*, vol. 48, pp. 716–726, 2013.

[9] A. Habbal, "Direct approach to the minimization of the maximal stress over an arch structure," *Journal of Optimization Theory and Applications*, vol. 97, no. 3, pp. 551–578, 1998.

[10] K. Kumarci, P. K. Dehkordy, I. Mahmodi et al., "Optimum shape in brick masonry arches under dynamic loads by cellular automata," *Journal of Civil Engineering*, vol. 37, no. 1, pp. 73–90, 2009.

[11] J. Park, Y.-H. Chun, and J. Lee, "Optimal design of an arch bridge with high performance steel for bridges using genetic algorithm," *International Journal of Steel Structures*, vol. 16, no. 2, pp. 559–572, 2016.

[12] M. Pouraminian and M. Ghaemian, "Shape optimisation of concrete open spandrel arch bridges," *Gradjevinar*, vol. 67, no. 12, pp. 1177–1185, 2015.

[13] H. P. Geering, *Optimal Control with Engineering Applications*, Springer, Berlin, Germany, 2007.

[14] L. S. Pontryagin, V. G. Boltyanskii, R. V. Gamkrelidze et al., *The Mathematical Theory of Optimal Processes*, Wiley-Interscience, New York, 1962.

[15] H. Laskowski, "Optimal design of structural elements as a control theory problem," *Technical Transactions. Civil Engineering*, vol. 114, no. 6, pp. 119–134, 2017.

[16] D. Kropiowska, *Selected problems of the optimal design of bar systems within the formal structure of the minimum principle*, Cracow University of Technology Publishing House, Cracow, 2016.

[17] L. Mikulski, "Control structure in optimization problems of bar systems," *International Journal of Applied Mathematics and Computer Science*, vol. 14, no. 4, pp. 515–529, 2004.

[18] H. Laskowski and L. Mikulski, "Control Theory in Composite Structure Optimizing," *Measurement Automation Monitoring*, vol. 55, no. 6, pp. 346–351, 2009.

[19] EN 1991-2 Eurocode 1:Actions on Bridges-Part 2: Traffic loads on bridges.

[20] G. Rakowski and R. Solecki, *Curved bars. Statical analysis*, Arkady, Warszawa, 1965.

[21] A. Gawecki, *Mechanics of materials and bar structures*, Poznan University of Technology Publishing House, Poznan, 1998.

[22] O. von Stryk, *Numerical hybrid optimal control and related topics [Dissertation, thesis]*, Technische Universität München, 2000.

[23] O. von Stryk, "Users guide for Dircol (Version 2.1): a direct collocation method for the numerical solution of optimal control problems," Simulation and Systems Optimization Group, Technische Universität Darmstadt, 2002.